Separation Science and Technology
Publication details, including instructions for authors and subscription information:
http://www.informaworld.com/smpp/title~content=t713708471

Block Copolymer Photo-Grafted Poly(Ethylene Terephthalate) Capillary Pore Membranes Distinctly Switchable by Two Different Stimuli

Christian Geismann[a]; Falk Tomicki[a]; Mathias Ulbricht[a]
[a] Lehrstuhl für Technische Chemie II, Universität Duisburg-Essen, and CeNIDE - Centre for Nanointegration Duisburg-Essen, Essen, Germany

To cite this Article Geismann, Christian , Tomicki, Falk and Ulbricht, Mathias(2009) 'Block Copolymer Photo-Grafted Poly(Ethylene Terephthalate) Capillary Pore Membranes Distinctly Switchable by Two Different Stimuli', Separation Science and Technology, 44: 14, 3312 — 3329
To link to this Article: DOI: 10.1080/01496390903212755
URL: http://dx.doi.org/10.1080/01496390903212755

Separation Science and Technology, 44: 3312–3329, 2009

ISSN: 0149-6395 print/1520-5754 online
DOI: 10.1080/01496390903212755

Taylor & Francis
Taylor & Francis Group

Block Copolymer Photo-Grafted Poly(Ethylene Terephthalate) Capillary Pore Membranes Distinctly Switchable by Two Different Stimuli

Christian Geismann, Falk Tomicki, and Mathias Ulbricht
Lehrstuhl für Technische Chemie II, Universität Duisburg-Essen, and CeNIDE – Centre for Nanointegration Duisburg-Essen, Essen, Germany

Abstract: Track-etched poly(ethylene terephthalate) capillary pore membranes with a pore diameter of 690 nm were functionalized via photo-initiated "living" radical graft polymerization with block copolymers of acrylic acid and N-isopropylacrylamide. Preadsorbed xanthone was more efficient than benzophenone in order to achieve higher grafting efficiency and "living" character, including the option to reinitiate a grafted homopolymer to obtain grafted diblock copolymers. Characterizations were mainly done with water flux and dextran diffusion experiments at temperatures below and above the lower critical solution temperature (32°C) of poly(N-isopropylacrylamide) and pH values below and above the pK_a value (4.5) of poly(acrylic acid). Block sequences and relative block lengths were identified to obtain stimuli-responsive membranes which have no measurable water flux and allow only low dextran diffusion rates at 25°C and pH 7 ("closed state"), and which reversibly open their pores by either increase of temperature or decrease of pH, or by the combination of both stimuli.

Keywords: Capillary pore membrane, iniferter, photo-grafting, polymer, stimuli-responsive, surface modification

Received 31 October 2008; accepted 26 April 2009.

Address correspondence to Mathias Ulbricht, Lehrstuhl für Technische Chemie II, Universität Duisburg-Essen, and CeNIDE – Centre for Nanointegration Duisburg-Essen, 45141 Essen, Germany. Tel.: +49-201–183 3151; Fax: +49-201–183 3147. E-mail: mathias.ulbricht@uni-due.de

INTRODUCTION

Stimuli-responsive polymers are known to undergo well-defined changes in their properties, like shape or volume as function of environmental conditions such as, temperature or pH value (1,2). Materials based on such "smart" polymers offer very promising perspectives in a variety of applications including drug delivery, sensor systems, and membrane technology (3,4). Poly-(N-isopropylacrylamide) (PNIPAAm), a prominent thermoresponsive polymer exhibits a lower critical solution temperature (LCST) in water. At temperatures below 32°C, the polymer chains are very well hydrated, whereas the polymer chains collapse as soon as the temperature is increased above this value (1,5). Poly(acrylic acid) (PAA), has a very pronounced change of its molecular size or degree of swelling in water upon protonation/deprotonation of the carboxyl side groups; the acid constant (pK_a) is about 4.5 (6). Interesting applications of macroscopic "smart" hydrogels are, for example, sealing materials based on weakly cross-linked PAA (6), and matrices for reversible immobilization of biomacromolecules based on weakly cross-linked PNIPAAm (7). The effect of a reversible volume change can also be applied to small channel structures in order to create novel valves (8). Layers of stimuli-responsive polymers anchored to the walls of isocylindrical polymer membrane pores via surface-selective "grafting-from" can serve as a model for such actuators (4,9,10). Also, such functionalized polymer membranes could be directly used to fulfill various functions in "lab-on-a-chip" systems, e.g., as "smart" barrier in switchable reservoirs for controlled drug release (11,12). Of particular scientific and technical interest is the creation of grafted block copolymer structures which consist of two polymers responding to different stimuli (13–15). Such block copolymers can also be formed by the "living" radical, sequential photo-grafting method. Here, the recombination of a growing polymer chain radical and a photoinitiator-derived radical (semipinacol radical, e.g., from benzophenone or xanthone) yields an aromatic ketyl end-group, which can be cleaved again by UV irradiation (15–17).

This work is an extension of our previous research on photo-initiated "grafting-from", in which the "type II" photo-initiator benzophenone (BP) very efficiently creates a starter radical on the polymer surface by hydrogen abstraction; this method had proven to be very versatile to prepare various different composite membranes, e.g., for pervaporation or ultrafiltration, or for applications as membrane adsorber. More details on this and other combinations of photochemistry and polymer membranes can be found in a recent review (18). Here we describe the synthesis of PAA and PNIPAAm co-grafted polyethyleneterephthalate (PET) track-etched membrane (TEM) pores via UV initiated living "radical", sequential graft copolymerization. Using such isoporous membranes,

here with a pore diameter of 690 nm, enable a much more detailed analysis of grafted layer thickness and its response to stimuli as compared with the previous work of two other groups where microfiltration membranes with rather irregular pore morphology had been used for similar surface functionalizations (15,17). It had been demonstrated in detail by various characterization methods (in particular, scanning electron microscopy, gas flow/pore dewetting, and liquid permeability measurements) that these PET TEM have a very narrow pore size distribution and quite regular cyclindrical pore shape over the entire membrane thickness; the possible reasons for irregularities which can occasionally be seen by scanning electron microscopy and which may cause small experimental errors had been comprehensively discussed in previous publications (9,10). The analysis of grafted layer thickness is then based on the water permeability of the photo-grafted membranes at combinations of pH values and temperatures above and below the pK_a of PAA and the LCST of PNIPAAm, respectively; this methodology had been described before for PET TEM with grafted homo polymers (9,10). Furthermore, the diffusion of dextran through the novel PAA and PNIPAAm co-grafted membranes at varied conditions is also analyzed.

EXPERIMENTAL

Materials

PET track-etched capillary pore membranes with nominal pore diameters of 400 nm were purchased from Oxyphen (Dresden, Germany). The actual pore diameter of this membrane had been determined via gas/flow pore dewetting porometry to be 690 nm at a very narrow size distribution; pore density is $7.6 \times 10^7\,cm^{-2}$, and membrane thickness is 23 μm (10). Solvents and reagents of analytical grade for preparation of buffer solutions were commercial products and were used as received. N-Isopropylacrylamide (NIPAAm) was purchased from Acros (Geel, Belgium) and used without further purification. Acrylic acid (AA), benzophenone (BP), xanthone, and dextran, labeled with fluorescein isothiocyanate (FITC dextran, average molar mass) were from Fluka (Steinheim, Germany). Water purified with a Milli-Q system from Millipore (Eschborn, Germany) was used for all the experiments.

Photo-Initiated Graft-Copolymerization

Influences of experimental conditions on efficiency of photo-grafting in PET membrane pores had been analyzed in detail before (9,10). Here

we focus on sequential photo-grafting. As a reference, statistical copolymers consisting of both monomers were grafted using the same procedure as described before (9,10). Pre-coating of the membranes by adsorption of the photo-initiator, i.e., BP or xanthone, was done with solutions in ethanol/water (10:1) with a concentration 50 mM for 60 min, followed by a quick rinse with the pure solvent and subsequent drying. Solutions of AA or NIPAAm in water with concentrations of 50 or 100 g/L were prepared and de-aerated by bubbling with pure nitrogen for 20 min immediately before contact with the membranes. The pre-coated membranes were placed between two filter papers, put in a Petri dish with the monomer solution and covered tightly with a smaller Petri dish to seal to the atmosphere. This glass also acted as deep-UV filter. The samples were placed in the center on the bottom of a reaction chamber built around an UVAPrint lamp (Dr. Hoenle AG, Gräfelfing, Germany) and then immediately irradiated (effective intensity reaching the membrane was about 7.5 mW/cm^2). Irradiation time was varied between 5 and 10 min. Thereafter, the membranes were first washed with water at room temperature for 30 min, then with methanol at room temperature for another 30 min, then dried at 45°C overnight, and finally weighed to determine the degree of graft-polymer modification (DG). DG was calculated according to:

$$\mathrm{DG} = \frac{m_{\mathrm{gr}} - m_0}{m_0} \cdot \frac{m_{\mathrm{sp,A}}}{A_{\mathrm{sp}}} \tag{1}$$

with m_0 (g) as initial sample weight, m_{gr} (g) weight after modification, $m_{\mathrm{sp,A}}$ (g/m^2) specific weight of the membrane (per outer surface area), and A_{sp} (m^2/m^2) specific surface area of the membrane.

The grafted copolymer composition was varied by the ratio of the monomers in the reaction mixture (total concentration 50 g/L). These membranes were labeled according to the ratio of monomers, P(A-N) aa-bb, where aa and bb represent the mass ratio of the two monomers.

For block copolymer grafting, photo-initiator was pre-adsorbed before the first grafting procedure (cf. above). After weighing, the membranes were immersed in a second monomer solution and then the same procedure as described above followed. It should be noted that no additional photo-initiator was added before the second step. These membranes were named after their block composition calculated from DG values obtained after the first and the second steps, PA-PN aa-bb (first block PAA, second block PNIPAAm) or PN-PA aa-bb (inverted block sequence), respectively. Membranes prepared with xanthone as

photoinitiator were labeled as those before, but using a prefix, i.e., x-PA-PN aa-bb.

Membranes PA-PN-5-95b, xPA-PN-7-93 and xPN-PA-83-17 had been prepared at least in triplicate, the variation coefficient for DG after 1st and 2nd steps was always less than 20%; this is significantly larger than typical data for 1-step photo-grafting (9,10).

Membrane Hydraulic Permeability and Calculation of Effective Pore Diameter/Grafted Layer Thickness

Flux measurements were done using stirred cells with 3 mL volume and 1.77 cm^2 active membrane area (Amicon Model 8003, Millipore), and the trans-membrane pressure was adjusted by the height of a water reservoir above the membrane (25 cm). The temperature of the reservoir contents was maintained at 25 and 45°C, respectively, using a thermostat (Julabo, Seelbach, Germany) and the Amicon cell was kept in a water bath also kept at the same temperature. The measurements were carried out with ultra pure water (pH 5.6), with water adjusted to pH 2 by using dilute HCl, of with buffers (20 mM citrate pH 2.0, 20 mM phosphate pH 7.0). Permeability resulted from dividing the flux by the trans-membrane pressure, and the pore sizes of the membranes were calculated from the permeability data by using the equation of Hagen-Poiseuille:

$$\frac{V}{\Delta t} = \frac{\pi \cdot \Delta P \cdot r^4}{8 \cdot \eta \cdot L} \tag{2}$$

where V is the volume of the permeate relating to a single cylindrical membrane pore, Δt is the time, ΔP is the trans-membrane pressure, r is the pore radius, η is the viscosity of water, and L is the capillary length, i.e., the membrane thickness. This equation is valid assuming a cylindrical geometry of the membrane pores and equal sizes of all the pores—this assumption is justified with the PET TEM used in this work because the same membranes as those extensively characterized before have been used (10). The first result is the effective hydrodynamic pore diameter, d_h (=2·r). The thickness of the grafted layer on the pore wall, l_h, can be calculated as the difference between the pore radius of the unmodified membrane and the pore radius of the functionalized membrane. Here we assume an even functionalization of the entire pore surface—the results reported in our recent paper on photo-grafted homopolymers in PET pores indicate that this assumption is justified (10).

Diffusion Experiments

A custom-made glass diffusion cell, consisting of two stirred half-cells (for liquid volumes of 140 mL) and a connector/membrane holder (for a membrane diameter of 40 mm) was used. The membrane was fixed in the holder, and the cell was tightly assembled. Then the two half-cells were filled at the same time with identical volumes of 140.0 mL (in order to avoid pressure-driven transport through the membrane), the "source" half-cell with a solution of FITC dextran (0.1 g/L) in the respective buffer (citrate buffer pH 2.0, or phosphate buffer pH 7.0), the "drain" half-cell with the plain buffer. Both solutions had been tempered to the desired temperature (25 or 45°C) before. The diffusion cell was immersed in a temperature-controlled water bath kept at the desired temperature. After constant time intervals, samples of 4 mL were taken out from both half-cells, and the concentrations were measured using a fluorescence spectrometer Cary Eclipse from Varian based on a calibration curve for FITC dextran in the respective buffer ($\lambda_{ex} = 492$ nm, $\lambda_{em} = 518$ nm). The solutions were then immediately put back into the respective cells. The diffusion coefficient D was calculated according to:

$$D = \frac{\Delta N \cdot x}{\Delta t \cdot A \cdot c} \tag{3}$$

where ΔN (mol) is the amount of dextran diffused from the "source" to the "drain" between two measurements (calculated from concentrations and liquid volumes), x is the membrane thickness (23 μm), Δt (h) is the time difference between two measurements, A is the outer surface pore area, i.e., the membrane area multiplied by surface porosity ($12.5 \times 0.12 = 1.5\,cm^2$), and c (mol/m^3) is the average difference of the molar dextran concentration for the period between the two measurements (calculated from measured "source" and "drain" concentrations). Average values of D for the first 2 hours were calculated. After the end of the experiment, the cell was emptied, both half-cells rinsed with a buffer, and another experiment at different conditions was started.

In preliminary experiments with varied settings of the magnetic stirrer, a high enough stirring speed had been identified where measured D was not significantly influenced by stirring conditions. Due to the cell geometry, a more precise description of mixing in the boundary layers is not possible; and estimations of mass transfer coefficients had not been performed. Due to additional mass transfer resistance in the boundary layers of the membrane, only effective diffusion coefficients D_{eff} are reported and discussed in terms of changes of membrane resistance toward the solute transport. Control experiments have shown that

the permeability of the membranes did not change due to pore blocking by the solute or restricted pore closing by reduced flexibility of the grafted layers, because repeating the first experiment after a series of four experiments under varied conditions gave identical values of D_{eff} within the range of experimental error (+10%).

RESULTS AND DISCUSSION

Membrane Functionalization

An overview of the functionalization results is given in Table 1. As a reference for the preparation and the characterization of grafted block copolymers, grafted random copolymers consisting of both functional monomers were prepared using otherwise the same procedure, including BP as photo-initiator, as described before (9,10). Similar values for the three compositions at the same total monomer concentration had been achieved, with somewhat lower DG for the highest content of AA in the monomer mixture.

The composition of the sequentially prepared membranes by using BP was varied by different irradiation times for each modification step and by the sequence of grafting of the two functional monomers. Monomer concentration was kept constant, except for one experiment. DG in the first step could be adjusted by UV irradiation time at constant monomer concentration, but similar to previous work (9,10) no linear dependency was found. Similar to the results for random copolymers, AA had a lower reactivity than NIPAAm under the specific functionalization conditions. In all cases, a significant increase in DG was obtained after the second grafting step. In addition, control experiments performed with UV irradiation of the membranes in monomer solutions without pre-coated photo-initiator yielded only negligible DG values. Due to the surface immobilization by pre-adsorption in the first step, the BP amounts in the monomer solution were very low. Consequently, in the second step, essentially only initiator groups covalently bound to the grafted polymer chain ends were photo-reactive and used for the re-initiation of the graft copolymerisation of the second block. Therefore, the assignment of the grafted polymers as predominantly block copolymers seems to be justified. This is also in agreement with the conclusions from other studies (15–17). Xanthone was also applied as a photo-initiator because the results of Yang and Rånby (16) had suggested a higher efficiency for "living" radical polymerization than BP. Achieved total DG and block ratios were similar to the results with BP under the same conditions.

Table 1. Functionalized PET track-etched membranes, photo-grafting preparation conditions and degree of functionalization per specific surface area

Membrane	1st step		2nd step		Block ratio 1st/2nd (wt/wt)	Degree of functionalization DG (μg/cm^2)
	c (g/L)	t_{UV} (min)	c (g/L)	t_{UV} (min)		
P(A-N) 75-25	50	5	–	–	–	1.4
P(A-N) 50-50	50	5	–	–	–	1.9
P(A-N) 25-75	50	5	–	–	–	1.8
PA-PN 92-8	50	10	50	5	92/8	0.8
PA-PN 17-83	50	7.5	50	5	17/83	4.4
PA-PN 5-95a	50	5	50	5	5/95	3.6
PA-PN 5-95b	50	10	50	10	5/95	5.2
x-PA-PN 7-93	50	10	50	5	7/93	4.9
PN-PA 53-47	50	5	50	5	53/47	3.2
PN-PA 88-12	50	7.5	50	5	88/12	2.2
PN-PA 97-3	50	10	50	5	97/3	1.8
x-PN-PA 83-13	50	5	100	5	83/13	3.2

Effective Pore Size of Functionalized Membranes and Implications for Grafted Layer Structure

The evaluation of the effective pore size or hydrodynamic layer thickness of the grafted layers on the pore walls is based on several pre-conditions:

1. base membrane with cylindrical pores at narrow size distribution,
2. even coverage of the known specific surface area with grafted polymer under functionalization conditions which do not damage the base pore structure, and
3. control of solution conditions which have influence in grafted layer swelling and electrokinetic effects during flux measurements (10).

Because the identical base membrane and experimental conditions as compared to our previous work have been used in this study, all these pre-conditions are fulfilled.

Figure 1 shows the effective hydrodynamic layer thicknesses of random copolymer grafted membranes. A reversible swelling with increasing pH was observable for all membranes but the effect became slightly smaller with a decrease of the PAA content. A reversible deswelling with increasing temperature was clearly detected only for the larger PNIPAAm contents (monomer ratio 50/50 wt/wt or larger) and at low pH. At higher pH, the temperature response was very small. At lower PNIPAAm contents and low pH, the grafted layer thickness even increased slightly with increasing temperature. PAA and PNIPAAm have different response mechanisms to the stimuli pH and temperature. The conformation of PAA chains expands with the deprotonation of carboxyl groups (pH effect), and because of the underlying electrostatic and osmotic effects the magnitude of the response is approximately proportional to the carboxyl group density (1,6). The conformation of PNIPAAm is

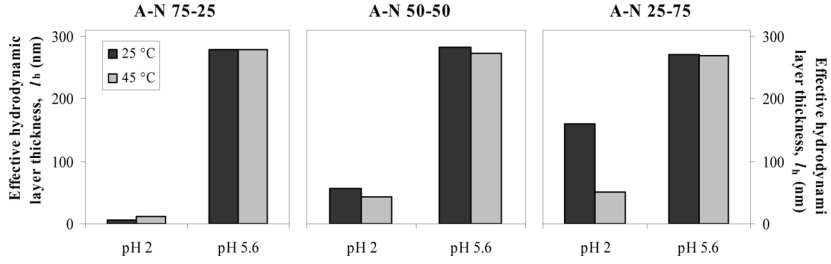

Figure 1. Effective hydrodynamic layer thicknesses of grafted random copolymer layers with different composition on PET membrane pore walls.

altered at the lower critical solution temperature (LCST) due to a change of the solvation state in water (temperature effect) (1,5,7). However, in contrast to PAA, this mechanism is very sensitive to contents of other functional groups in the polymer and to PNIPAAm sequence lengths. Too short PNIPAAm sequences (oligomers with less than 10 subsequent NIPAAm units) do not show LCST behavior (19). In addition, (multiple) hydrogen bonding can occur between PNIPAAm and protonated PAA segments (20), and this can lead to an "inverse" temperature response when compared with the LCST effect. Hence, instead of an increase of the overall degree of swelling at lower temperature (due to swelling of PNIPAAm segments below LCST), hydrogen bonds between PNIPAAm and PAA segments leads to a more compact structure of the entire hydrogel layer. This is even more reasonable because the swelling capacity of PAA (at high and low pH) is larger than that of PNIPAAm (at low temperature). Based on these mechanisms, all observations for the different polymer compositions – dominating pH effect, less pronounced temperature effect and "reverse" temperature response for the smallest NIPAAm contents – can be well explained. Also, under the used polymerization conditions in water (at moderate conversion of monomer in the pores), the reactivities of NIPAAm and AA seemed to be more similar than indicated by the copolymerization parameters determined in ethanol (21).

From Fig. 2 it can clearly be seen that the PAA-PNIPAAm membrane with a high PAA content (PA-PN 92-8) showed a "reverse" temperature effect for both measured pH values. The reasons have been discussed above, however, the effect of hydrogen bonding was stronger than for the random graft copolymers, i.e., observed at lower PNIPAAm content and also, to some extent, at higher pH. Nevertheless, an increase in pH from 2 to 5.6 caused a significant increase in the hydrodynamic layer thickness. For the PA-PN 17-83 membrane, despite the much higher proportion of PNIPAAm, the pH effect was still significant, while a temperature response just emerged. At an even larger ratio (PA-PN 5-95a), where the layer thickness could be altered largely by a change in temperature, the pH response still remained significant (Fig. 3). Here, both stimuli could change the pore diameter significantly, i.e., the temperature effect was superimposed by the pH effect. Further, independent of the degree of functionalization the layer thicknesses in the expanded state, i.e., at pH 5.6 and 25°C, were approximately constant for all investigated PAA-PNIPAAm membranes. Both of the last observations can be well explained by the up to 10 times larger degree of swelling of PAA (in ionized form at 25°C) in comparison to PNIPAAm (at 25°C) (22,23). It should be noted, that the pH-induced swelling would be even larger above the pH 5.6 of water used in this experiment (cf., e.g., refs. 9 and 22).

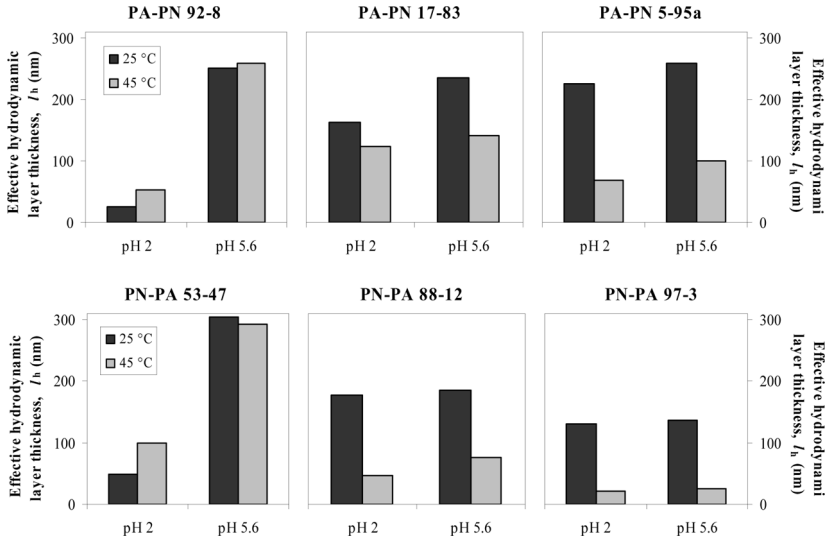

Figure 2. Effective hydrodynamic layer thicknesses of grafted PAA-PNIPAAm (top) and PNIPAAm-PAA (bottom) block copolymer layers on PET membrane pore walls.

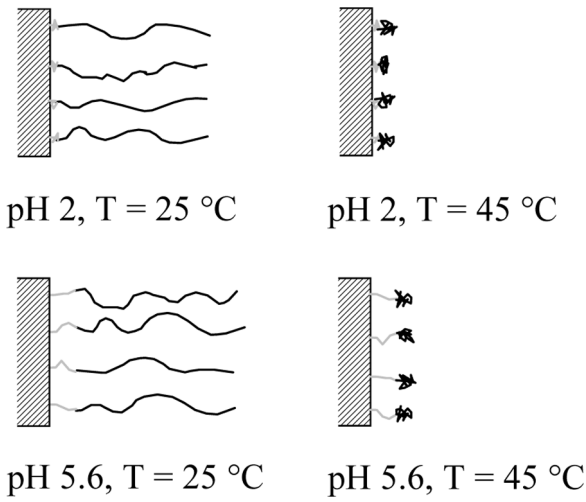

Figure 3. Schematic illustration of the functional principle of pore walls grafted with PAA-b-PNIPAAm block copolymers at high PNIPAAm proportion.

The results for an inverse block sequence (cf. Fig. 2) show that the "reverse" temperature effect—due to hydrogen bonding—was large even for a 50/50 PNIPAAm/PAA composition at low pH, while a pH dependency could clearly be observed. With increasing PNIPAAm content, the LCST-based response emerged at both pH values; however, the pH effect was very small or not observed. This latter result is clearly different from the finding for the other sequence (cf. Fig. 3). It is presumably due to the polydispersity of PNIPAAm chain lengths of the first block so that the overall effects of the swelling/deswelling transition of the shorter second PAA block were less distinct. Therefore, for this block copolymer sequence prepared with BP as photo-initiator no PNIPAAm/PAA ratio could be identified, where both stimuli yield large responses.

Based on the above results about the effects of block sequence, samples with grafted PAA-b-PNIPAAm block copolymers at a higher DG were prepared (cf. Table 1), in order to achieve complete pore blocking in the water-swollen state. Figure 4 shows the pore diameters of the membranes obtained by using the two different photo-initiators. It can clearly be seen that the use of xanthone led to a superior performance of the responsive membrane because the magnitude of pore size change increased from 80 to 150 nm (pH decrease, at 25°C) and from 150 to 220 nm (T increase, at pH = 5.6), respectively. This can be explained by a higher efficiency of the "living" graft copolymerization mechanism, i.e., more re-initiating by the ketyl-PAA chain ends and less uncontrolled initiation and growth reactions during the synthesis of both blocks. As already discussed above regarding the higher DG values under the same

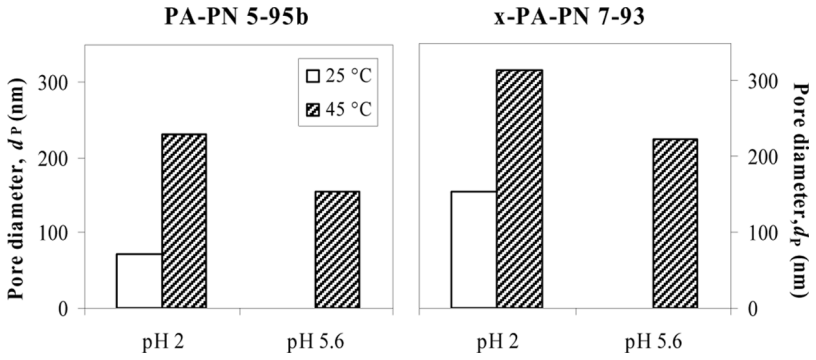

Figure 4. Influence of the photo-initiator on the filtration performance of PAA-b-PNIPAAm block copolymer grafted PET membranes at the same DG and block ratio (trans-membrane pressure $\Delta p = 2.4$ kPa); note that the values at pH 5.6 and 25°C were about zero, i.e., no water flux could be measured under the applied conditions; i.e., the pores were completely blocked.

conditions, this better control is also in line with the results of Yang and Rånby (16). The pores of this type of membrane could very effectively be opened and closed by both stimuli.

Using xanthone, the preparation of grafted PET membranes with the other sequence had also been attempted again; in addition, the concentration of NIPAAm in the second step had been increased (cf. Table 1). DG values and block ratios for these membranes were similar to the sample PN-PA-88-12 prepared using BP; the somewhat higher total DG and slightly higher PNIPAAm content could be due to both changes (different initiator and higher monomer concentration). Figure 5 summarizes results obtained from water flux measurements. This membrane was with respect to total DG and composition in between two PN-PA membranes which had been prepared using BP and which did not show a response to both stimuli (cf. Fig. 2); nevertheless, very clear and distinct switching behavior as a function of both pH and temperature was observed. This is a strong indication that the more versatile photo-initiator xanthone has changed the course of graft copolymerization to a more controlled mode. That the pH effects were larger than the temperature effects could be related to the composition of the copolymers. However, considering the expected much larger swelling/deswelling ratios of PAA as compared to PNIPAAm (cf. above), the full potential of the PAA block to change the effective pore size was not apparent in this membrane. This indicates that the effects of multiple hydrogen bonding and chain length polydispersity discussed above do also play a significant role for this membrane.

Diffusion experiments with dextran had been performed for both membranes prepared using xanthone as photo-initiator (Fig. 6). For both

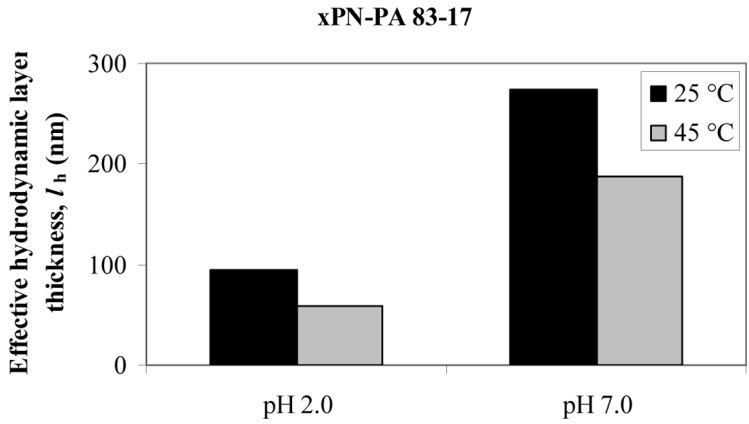

Figure 5. Effective hydrodynamic layer thicknesses of PNIPAAm-PAA block copolymer grafted PET membrane prepared using xanthone as photo-initiator.

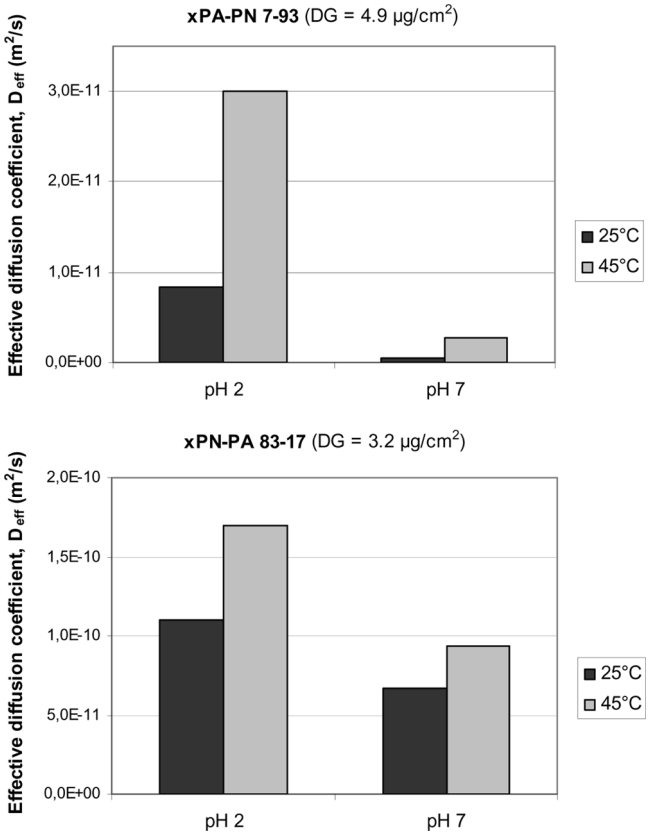

Figure 6. Effective diffusion coefficients for dextran with average molar mass of 4000 g/mol through two stimuli-responsive grafted block copolymer membranes based on track-etched PET as function of the combination of pH and temperature (for the unmodified PET TEM: D_{eff} (45°C, pH 7) = 4.4×10^{-10} m^2/s).

membranes, the changes of the diffusion rate as a function of pH and temperature were in qualitative agreement with the expectations based on the effective pore size deduced from water flux measurements (cf. Fig. 5, right, and Fig. 6). The values for the grafted PNIPAAm-b-PAA membrane were larger than for the grafted PAA-b-PNIPAAm membrane; this can be explained by the lower DG (all data were still significantly smaller than for the unmodified base membrane). However, the changes were also less pronounced, and this may be related with too less well-defined block copolymer/separate layer structure for this sequence of stimuli-responsive copolymer discussed above. On the other hand, it is remarkable that with the PNIPAAm-b-PAA membrane, the diffusion

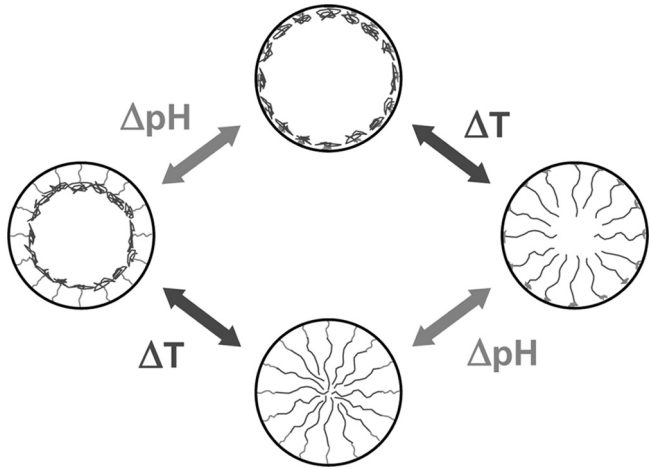

Figure 7. Schematic illustration of the reversible pore opening/blocking, induced by two different stimuli, for PET pores with grafted PAA-b-PNIPAm.

rate for the relatively small macromolecule (hydrodynamic radius about 3 nm (7)) could be "switched" by about two orders of magnitude. The function of the novel membranes with this block sequence is schematically shown in Fig. 7.

When comparing the results from water flux measurement and solute diffusion for the two PET TEM sequentially photo-grafted using xanthone as photo-initiator (cf. Fig. 4, right and Fig. 5 vs. Fig. 6), we note a significant difference: While for hydraulic permeability the largest changes are observed for the transition from "closed" state (at high pH and low temperature), the largest changes in the diffusion experiments occur relative to the most open state of the pores (at low pH and high temperature). The latter effect may partially be influenced by the higher solute diffusion rate at higher temperature. However, for the "closed" state of the pores, diffusion of the small solute is still possible through the space between the grafted polymer chains (additional experiments with dextrans of larger molar mass, i.e., 70.000 g/mol corresponding to a hydrodynamic diameter of about 12 nm, revealed that size exclusion was still not complete). In contrast, viscous flow is completely blocked (at least for relatively low pressure differences).

These interpretations are also supported by results of a recent comparative study: photo-grafted PNIPAAm PET TEM obtained by the same procedure as used in this work have been compared with grafted materials made from the same base membranes, but using highly controlled surface-initiated atom radical transfer polymerization (ATRP) (24).

With surface-initiated ATRP, grafted layers with a much higher polymer density in swollen state ($0.37\,g/cm^3$ vs. $0.06\,g/cm^3$) and a much lower swelling/deswelling ratio ($\sim$3 vs. $\sim$16), both as compared to photo-grafting, have been obtained. This implies that the photo-grafted layers obtained with photo-grafting are in the "mush-room" regime, i.e., the chains have a large average distance and hence a very pronounced mobility. This is in line with the observed diffusive permeability of macromolecules through pores which are "closed" for viscous flow at low pressure. Also the deviations in switching behavior attributed to bonds between segments of different polymer blocks can be explained (this could occur even in an ideal block copolymer layer because at low grafting density "back-folding" of chains from the outer layer into the inner layer will be possible). In contrast, the highly controlled surface-initiated ATRP from PET TEM allows synthesis of grafted layers with high density, including block copolymer layers with more distinct switching behavior (25).

CONCLUSION

In conclusion, pore walls of PET capillary pore membranes were functionalized with block copolymer chains consisting of two polymers responding to different stimuli. Such valve functionality could only be achieved by a controlled, "living" graft copolymerization. The response in terms of effective layer thickness could be tuned by synthesis conditions and precisely be measured using membrane permeability. The permeabilities of membranes with suited block copolymer sequence and ratio, as well as a sufficient degree of functionalization were distinctly switchable either by a change in pH or in temperature. The type of photo-initiator had a significant effect onto the extent and the controllability of this response to stimuli; xanthone with a higher probability for chain propagation by the "living" mechanism allows higher efficiency of selective re-initiation and thus a better control of polydispersity and higher yield of grafted block copolymers. This concept can be easily adapted to other membrane pore sizes and shapes or fluidic channel geometries, and it has therefore large potential for the development of novel membrane- or chip-based separation technologies.

ACKNOWLEDGEMENT

The financial support of the work by the Deutsche Forschungsgemeinschaft (DFG U1 113/6-1) and the skilled technical support of the experiments by Claudia Schenk is gratefully acknowledged.

REFERENCES

1. Shibayama, M.; Tanaka, T. (1993) Volume phase-transition and related phenomena of polymer gels. *Adv. Polym. Sci.*, *109*: 1–62.
2. Hoffman, A.S. (1995) Intelligent polymers in medicine and biotechnology. *Macromol. Symp.*, *98*: 645–664.
3. Kumar, A.; Srivastava, A.; Galaev, I.Y.; Mattiasson, B. (2007) Smart polymers: Physical forms and bioengineering applications. *Prog. Polym. Sci.*, *32*: 1205–1237.
4. Ulbricht, M. (2006) Advanced functional polymer membranes. *Polymer*, *47*: 2217–2262.
5. Rzaev, Z.M.O.; Dincer, S.; Piskin, E. (2007) Functional copolymers of N-isopropylacrylamide for bioengineering applications. *Prog. Polym. Sci.*, *32*: 534–595.
6. Wack, W.; Ulbricht, M. (2007) Method and model for the analysis of gel blocking effects during the swelling of polymeric hydrogels. *Ind. Chem. Eng. Res.*, *46*: 359–364.
7. Fänger, C.; Wack, H.; Ulbricht, M. (2006) Macroporous poly (N-isopropylacrylamide) hydrogels with adjustable size "cut-off" for the efficient and reversible immobilization of biomacromolecules. *Macromol. Biosci.*, *6*: 693–402.
8. Beebe, D.J.; Moore, J.S.; Bauer, J.M.; Yu, Q.; Liu, R.H.; Devadoss, C.; Jo, B.H. (2000) Functional hydrogel structures for autonomous flow control inside microfluidic channels. *Nature*, *404*: 588–590.
9. Geismann, G.; Ulbricht, M. (2005) Photoreactive functionalization of poly (ethylene terephthalate) track-etched pore surfaces with "smart" polymer systems. *Macromol. Chem. Phys.*, *206*: 268–281.
10. Geismann, G.; Yaroshchuk, A.; Ulbricht, M. (2007) Permeability and electrokinetic characterization of poly(ethylene terephthalate) capillary pore membranes with grafted temperature-responsive polymers. *Langmuir*, *23*: 76–83.
11. Eddington, D.T.; Beebe, D.J. (2004) Flow control with hydrogels. *Adv. Drug Deliv. Rev.*, *56*: 199–210.
12. de Jong, J.; Lammertink, R.G.H.; Wessling, M. (2006) Membranes and microfluidics: A review. *Lab On a Chip*, *6*: 1125–1139.
13. Chen, G.; Hoffman, A.S. (1995) Graft-copolymers that exhibit temperature-induced phase-transitions over a wide-range of pH. *Nature*, *373*: 49–52.
14. Zhou, S.; Chu, B. (1998) Synthesis and volume phase transition of poly(methacrylic acid-*co*-*N*-isopropylacrylamide) microgel particles in water. *J. Phys. Chem. B*, *102*: 1364–1371.
15. Peng, T.; Cheng, Y.L. (2001) PNIPAAm and PMAA co-grafted porous PE membranes: Living radical co-grafting mechanism and multi-stimuli responsive permeability. *Polymer*, *42*: 2091–2100.
16. Yang, W.; Rånby, B. (1996) Radical living graft polymerization on the surface of polymeric materials. *Macromolecules*, *29*: 3308–3310.
17. Ma, H.; Davis, R.H.; Bowman, C.N. (2000) A novel sequential photoinduced living graft polymerization. *Macromolecules*, *33*: 331–335.

18. He, D.; Susanto, H.; Ulbricht, M. (2009) Photo-irradiation for preparation, modification and stimulation of polymeric membranes. *Progr. Polym. Sci.*, *34*: 62–98.
19. Plunkett, K.N.; Zhi, X.; Moore, J.S.; Leckband, D.E. (2006) PNIPAM chain collapse depends on the molecular weight and grafting density. *Langmuir*, *22*: 4259–4266.
20. Bergbreiter, D.E.; Case, B.L.; Liu, Y.S.; Caraway, J.W. (1998) Poly(N-isopropylacrylamide) soluble polymer supports in catalysis and synthesis. *Macromolecules*, *31*: 6053–6062.
21. Xue, W.; Champ, S.; Huglin, M.B. (2000) Observations on some copolymerisations involving N-isopropylacrylamide. *Polymer*, *41*: 7575–7581.
22. Philippova, O.E.; Hourdet, D.; Audebert, R.; Khokhlov, A.R. (1997) pH-responsive gels of hydrophobically modified poly(acrylic acid). *Macromolecules*, *30*: 8278–8285.
23. Díez-Peña, E.; Quijada-Garrido, I.; Barrales-Rienda, J.M. (2002) Hydrogen-bonding effects on the dynamic swelling of (PNIPAAm-co-MAA) copolymers. A case of autocatalytic swelling kinetics. *Macromolecules*, *35*: 8882–8888.
24. Friebe, A.; Ulbricht, M. (2007) Controlled pore functionalization of poly (ethylene terephthalate) track-etched membranes via surface-initiated atom transfer radical polymerisation. *Langmuir*, *23*: 10316–10322.
25. Friebe, A.; Ulbricht, M. (2009) Cylindrical pores responding to two different stimuli via surface-initiated atom transfer radical polymerization for synthesis of grafted diblock copolymers. *Macromolecules*, *42*: 1838–1848.